



## Performance behavior of prediction filters for respiratory motion compensation in radiotherapy

Jöhl, Alexander ; Berdou, Yannick ; Guckenberger, Matthias ; Klöck, Stephan ; Meboldt, Mirko ; Zeilinger, Melanie ; Tanadini-Lang, Stephanie ; Schmid Daners, Marianne

**Abstract:** In radiotherapy, tumors may move due to the patient's respiration, which decreases treatment accuracy. Some motion mitigation methods require measuring the tumor position during treatment. Current available sensors often suffer from time delays, which degrade the motion mitigation performance. However, the tumor motion is often periodic and continuous, which allows predicting the motion ahead. **Method and Materials:** A couch tracking system was simulated in MATLAB and five prediction filters selected from literature were implemented and tested on 51 respiration signals (median length: 103 s). The five filters were the linear filter (LF), the local regression (LOESS), the neural network (NN), the support vector regression (SVR), and the wavelet least mean squares (wLMS). The time delay to compensate was 320 ms. The normalized root mean square error (nRMSE) was calculated for all prediction filters and respiration signals. The correlation coefficients between the nRMSE of the prediction filters were computed. **Results:** The prediction filters were grouped into a low and a high nRMSE group. The low nRMSE group consisted of the LF, the NN, and the wLMS with a median nRMSE of 0.14, 0.15, and 0.14, respectively. The high nRMSE group consisted of the LOESS and the SVR with both a median nRMSE of 0.34. The correlations between the low nRMSE filters were above 0.87 and between the high nRMSE filters it was 0.64. **Conclusion:** The low nRMSE prediction filters not only have similar median nRMSEs but also similar nRMSEs for the same respiration signals as the high correlation shows. Therefore, good prediction filters perform similarly for identical respiration patterns, which might indicate a minimally achievable nRMSE for a given respiration pattern.

DOI: <https://doi.org/10.1515/cdbme-2017-0090>

Posted at the Zurich Open Repository and Archive, University of Zurich

ZORA URL: <https://doi.org/10.5167/uzh-143383>

Journal Article

Published Version



The following work is licensed under a Creative Commons: Attribution-NonCommercial-NoDerivatives 4.0 International (CC BY-NC-ND 4.0) License.

Originally published at:

Jöhl, Alexander; Berdou, Yannick; Guckenberger, Matthias; Klöck, Stephan; Meboldt, Mirko; Zeilinger, Melanie; Tanadini-Lang, Stephanie; Schmid Daners, Marianne (2017). Performance behavior of pre-

diction filters for respiratory motion compensation in radiotherapy. *Current Directions in Biomedical Engineering*, 3(2):429-432.  
DOI: <https://doi.org/10.1515/cdbme-2017-0090>

Alexander Jöhl\*, Yannick Berdou, Matthias Guckenberger, Stephan Klöck, Mirko Meboldt, Melanie Zeilinger, Stephanie Tanadini-Lang and Marianne Schmid Daners

# Performance behavior of prediction filters for respiratory motion compensation in radiotherapy

**Abstract:** Introduction: In radiotherapy, tumors may move due to the patient's respiration, which decreases treatment accuracy. Some motion mitigation methods require measuring the tumor position during treatment. Current available sensors often suffer from time delays, which degrade the motion mitigation performance. However, the tumor motion is often periodic and continuous, which allows predicting the motion ahead. Method and Materials: A couch tracking system was simulated in MATLAB and five prediction filters selected from literature were implemented and tested on 51 respiration signals (median length: 103 s). The five filters were the linear filter (LF), the local regression (LOESS), the neural network (NN), the support vector regression (SVR), and the wavelet least mean squares (wLMS). The time delay to compensate was 320 ms. The normalized root mean square error (nRMSE) was calculated for all prediction filters and respiration signals. The correlation coefficients between the nRMSE of the prediction filters were computed. Results: The prediction filters were grouped into a low and a high nRMSE group. The low nRMSE group consisted of the LF, the NN, and the wLMS with a median nRMSE of 0.14, 0.15, and 0.14, respectively. The high nRMSE group consisted of the LOESS and the

SVR with both a median nRMSE of 0.34. The correlations between the low nRMSE filters were above 0.87 and between the high nRMSE filters it was 0.64. Conclusion: The low nRMSE prediction filters not only have similar median nRMSEs but also similar nRMSEs for the same respiration signals as the high correlation shows. Therefore, good prediction filters perform similarly for identical respiration patterns, which might indicate a minimally achievable nRMSE for a given respiration pattern.

**Keywords:** radiotherapy, tumor motion, respiration, prediction filter

<https://doi.org/10.1515/cdbme-2017-0090>

## 1 Introduction

In radiotherapy, some tumors in the thorax or abdomen move during the treatment. There are several approaches to cope with moving tumors, the conventional approach being the expansion of the target volume to be irradiated. The expansion ensures the radiation dose coverage of the tumor, but also leads to an increase of the radiation dose to the healthy tissue surrounding the tumor. In this study, we consider tumors that move due to the respiration of the patients.

Alternative approaches for these cases are gating, breath-hold gating, and dynamic tracking [4]. In gating, the respiration is measured during treatment and only when the respiration is in a predefined window (e.g. respiration phase), the radiation beam is switched on. In breath-hold gating, the patient holds the breath for a given time interval and only then the beam is switched on. In dynamic tracking, either the beam source is moved [5, 9], the beam itself is modified [3] or the patient is moved to compensate for the tumor motion [6].

These approaches require monitoring the position of the tumor or a surrogate, which allows estimating the tumor position. Unfortunately, the sensors and actuators currently

\*Corresponding author: **Alexander Jöhl:** Product Development Group Zurich, Department of Mechanical and Process Engineering, ETH Zurich, CLA G19.2 Tannenstrasse 3 8092 Zurich, Switzerland, e-mail: joehla@ethz.ch

**Yannick Berdou, Mirko Meboldt, Marianne Schmid Daners:** Product Development Group Zurich, Department of Mechanical and Process Engineering, ETH Zurich, Switzerland, e-mail: berdouy@ethz.ch, meboldtm@ethz.ch, marischm@ethz.ch.

**Melanie Zeilinger:** Institute for Dynamic Systems and Control, Department of Mechanical and Process Engineering, ETH Zurich, Switzerland, e-mail: mzeilinger@ethz.ch

**Matthias Guckenberger, Stephan Klöck, Stephanie Tanadini-Lang:** Department of Radiation Oncology, University Hospital Zurich, University of Zurich, Switzerland, e-mail: matthias.guckenberger@usz.ch, stephan.kloeck@usz.ch, stephanie.tanadini-lang@usz.ch.

available often suffer from time delays, which substantially decrease effectiveness of tracking and gating. However, time delays can potentially be compensated by applying prediction filters, which exploit the periodicity and continuity of the respiration to predict the respiration signal ahead.

In literature, various prediction filter approaches were proposed, which range from classical signal processing to machine learning approaches like neural networks. However, comparisons between the studies of the prediction filters are difficult, because different respiration data were used or the time delays differed. Therefore, a selection of prediction filters from literature was implemented in this work and applied to various respiratory motion data. The resulting prediction data allows analyzing the performance behaviors of the prediction filters.

## 2 Method and materials

### 2.1 Simulation setup

The prediction filters to be investigated were implemented in MATLAB (The MathWorks Inc., Natick, MA, USA). The sampling frequency of all the signals were 25 Hz. The time delay to be compensated was  $\delta = 8$  samples corresponding to 320 ms.

### 2.2 Respiration data set

The respiration data set consists of 51 signals from different patients (median length: 103 s). The respiration data are smooth scalar signals with a sampling frequency of 25 Hz. The signals are not normalized and therefore, vary in their amplitude from 1.5 mm to 19 mm with a median of 8.3 mm. The respiration frequency varies from 0.1 Hz to 0.4 Hz with a median of 0.2 Hz. Additionally, the maximum absolute speeds that occur in each signal were estimated by finite differences and taking the 97<sup>th</sup> percentile of the resulting absolute speed signal. The slowest maximum speed over the whole set is 2 mm/s and the fastest one is 22 mm/s (median of 8 mm/s). Analogously, the maximum absolute acceleration was estimated (90<sup>th</sup> percentile) and the slowest one is 5 mm/s<sup>2</sup> and the fastest is 53 mm/s<sup>2</sup> (median of 13 mm/s<sup>2</sup>).

### 2.3 Prediction filter

Five different prediction filters were implemented. In the following, all the prediction filters are described.

#### 2.3.1 Linear filter

The linear filter (LF) is a sliding window linear regression  $\hat{x}(k + \delta|k) = \mathbf{a}^T \mathbf{x}$ , where  $\mathbf{x}$  is the signal vector consisting of the  $n$  latest samples including the current sample  $x(k)$ , where  $k$  is the current time step, and  $\hat{x}(k + \delta|k)$  is the estimate of  $x$  in  $\delta$  time steps. The weights  $\mathbf{a}$  are determined by  $N$  pairs of a row vector  $\mathbf{x}_i$  and a scalar  $y_i$  using (1). The row vector  $\mathbf{x}_i$  (training vector) consists of  $n$  consecutive values of the respiration signal, while  $y_i$  (training response) is the value of the respiration signal  $\delta$  time steps ahead of the latest entry of  $\mathbf{x}_i$ .

$$\mathbf{a} = \left( \begin{pmatrix} \mathbf{x}_1 \\ \vdots \\ \mathbf{x}_N \end{pmatrix}^T \begin{pmatrix} \mathbf{x}_1 \\ \vdots \\ \mathbf{x}_N \end{pmatrix} \right)^{-1} \begin{pmatrix} \mathbf{x}_1 \\ \vdots \\ \mathbf{x}_N \end{pmatrix}^T \begin{pmatrix} y_1 \\ \vdots \\ y_N \end{pmatrix} \quad (1)$$

#### 2.3.2 Local regression

The local regression (LOESS) [8] prediction filter works similarly to the LF, but with additional steps before computing the weights. Only the  $r < N$  training vectors most “similar” to the current signal vector are used for computing the weights. The “similarity” is the inverse of the Euclidean distance between two vectors. In addition to this selection, the training vectors are weighted by their similarity to the current signal vector. The training vector weighting formula is:

$$w_i = \kappa \left( \frac{\|\mathbf{x}_i - \mathbf{x}\|}{h_r} \right) \quad i = 1, \dots, r \quad (2)$$

$$\text{where } \kappa(x) = \begin{cases} (1 - |x|^3)^3 & \text{if } |x| < 1 \\ 0 & \text{if } |x| \geq 1 \end{cases}$$

The scalar  $h_r$  is the largest distance between the  $r$  selected training vectors and the current signal vector. The training vectors are expanded into a training vector  $\mathbf{z}$  containing monomials up to a chosen order. For example a quadratic polynomial:

$$\mathbf{x}_i = [x_1, x_2, \dots, x_n] \rightarrow \mathbf{z}_i = [x_1, x_2, x_1 x_2, x_1^2, \dots, x_n^2] \quad (3)$$

The selected and expanded training vectors are then used to determine the weight vector  $\mathbf{a}$  for the prediction  $\hat{x}(k + \delta|k) = \mathbf{a}^T \mathbf{z}$ . The weights  $\mathbf{a}$  are determined by:

$$\mathbf{a} = \left( \begin{pmatrix} \mathbf{z}_1 \\ \vdots \\ \mathbf{z}_r \end{pmatrix}^T \mathbf{W} \begin{pmatrix} \mathbf{z}_1 \\ \vdots \\ \mathbf{z}_r \end{pmatrix} \right)^{-1} \begin{pmatrix} \mathbf{z}_1 \\ \vdots \\ \mathbf{z}_r \end{pmatrix}^T \mathbf{W} \begin{pmatrix} y_1 \\ \vdots \\ y_r \end{pmatrix} \quad (4)$$

$$\text{where } \mathbf{W} = \begin{pmatrix} w_1 & \dots & 0 \\ \vdots & \ddots & \vdots \\ 0 & \dots & w_r \end{pmatrix}$$

### 2.3.3 Support vector regression

The support vector regression (SVR) [2] prediction filter solves an optimization problem to find a function  $x = f(k) = \beta^T k + b$ .

$$\begin{aligned} \min_{\beta} \quad & \frac{1}{2} \beta^T \beta + C \sum_{i=1}^N (\xi_i + \xi_i^*) \\ \text{such that} \quad & x_i - (\beta^T k_i + b) \leq \varepsilon + \xi_i \\ & (\beta^T k_i + b) - x_i \leq \varepsilon + \xi_i^* \\ & \xi_i, \xi_i^* \geq 0 \quad \forall i \in \{1, \dots, N\} \end{aligned} \quad (5)$$

The main idea is to allow deviations of the function  $f$  at the training data  $k_i$  from the training response  $x_i$  without increasing the optimization cost. Only when the deviation is above the threshold  $\varepsilon$ , the cost increases. In formulation (5), the function  $f$  is linear. To achieve nonlinear functions, the data is transformed nonlinearly:  $x = \beta^T \phi(k) + b$ , where  $\phi: \mathbb{R}^n \rightarrow \mathbb{R}^m$ . The transformation may be computationally intensive, however the so-called dual of the optimization problem (5) can be used to find  $f$ . In the dual optimization problem, the training data  $k_i$  only appear in an inner product  $\phi(k_i)^T \phi(k_j)$ , which can be replaced by a kernel function  $k(k_i, k_j)$ . The kernel function used here was  $k(k_i, k_j) = \exp(-2\|k_i - k_j\|^2)$ . Then, the prediction is  $\hat{x}(k + \delta|k) = f(k + \delta)$ .

### 2.3.4 Wavelet least mean squares

The wavelet least mean squares (wLMS) [1] prediction filter works by wavelet decomposition up to a level  $J$ . Apply the equations (6)  $J$  times:

$$\begin{aligned} c_0(k) &= x(k), \quad c_{j+1}(k) = \frac{1}{2} \left( c_j(k - 2^j) + c_j(k) \right), \\ W_{j+1}(k) &= c_j(k) - c_{j+1}(k) \end{aligned} \quad (6)$$

Then there are  $J + 1$  levels, which represent the original signal:  $x(k) = W_1(k) + \dots + W_J(k) + c_J(k)$ . Each level can be considered to be a signal on its own to be predicted ahead. Therefore, all levels are predicted ahead with the LF prediction filter method and the resulting predictions are then combined to a prediction of the original signal.

$$\hat{x}(k + \delta|k) = \hat{W}_1(k + \delta|k) + \dots + \hat{c}_J(k + \delta|k) \quad (7)$$

### 2.3.5 Neural networks

The neural network (NN) [7] prediction filter takes the current signal vector  $x$  of length  $n$  and passes each component to the activation functions  $\phi(x) = \frac{2}{1 + \exp(-2x)} - 1$ , which are called input layer neurons. The hidden neurons layer consists of  $h$  activation functions, which each take the

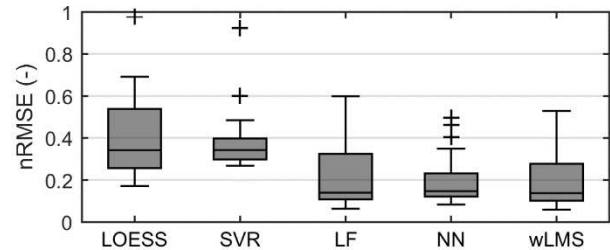


**Figure 1:** The distribution of the nRMSE of all the prediction filters visualized by their respective boxplots. The boxes show the 25<sup>th</sup> percentile, the median, and the 75<sup>th</sup> percentile. A data point is an outlier (+) if its distance from the respective percentile (25<sup>th</sup> or 75<sup>th</sup>) is larger than 1.5 times the box length.

weighted sum of the input layer results  $s_{i,\text{input}}$  and pass it through the activation function  $s_{j,\text{hidden}} = \phi(\sum_{i=1}^n a_{ji} s_{i,\text{input}} + a_{j,\text{bias}})$ . The output layer consists of one activation function receiving the outputs of the hidden layer  $\hat{x}(k + \delta|k) = \phi(\sum_{j=1}^h b_j s_{j,\text{hidden}} + b_{\text{bias}})$ . The NN weights  $a_{ji}$  and  $b_j$  are determined by  $N$  past pairs of training vectors  $x_i$  and training responses  $y_i$ . The weights are set by the training method “conjugate gradient backpropagation with Powell-Beale restarts”.

## 2.4 Analysis

The quality of the prediction filters was assessed by the normalized root mean square error (nRMSE), see (8). The resulting values are dimensionless and show, how well the prediction filter mitigates the time delay. For the nRMSE results the Friedman-test was used. The post-hoc tests used the Scheffé method.

$$\text{nRMSE} = \sqrt{\frac{\sum_{k=1}^M (\hat{x}(k + \delta|k) - x(k + \delta))^2}{\sum_{k=1}^M (x(k) - x(k + \delta))^2}} \quad (8)$$

## 3 Results

The nRMSE of all the prediction filters are shown in Figure 1. The LOESS and the SVR showed higher medians than the LF, NN, and wLMS. Therefore, the prediction filters can be grouped into a high nRMSE group (LOESS, SVR) and a low nRMSE group (LF, NN, wLMS). The Friedman-test showed that there was at least one significant difference ( $p < 0.0001$ ) in the median nRMSEs of the prediction filters. The post-hoc tests (Scheffé) only showed significant differences between the high nRMSE and the low nRMSE groups of prediction filters. The significant post-hoc tests p-values were all below 0.0001.

**Table 1:** The Pearson correlations of the nRMSE of each prediction filter: local regression (LOESS), support vector regression (SVR), linear filter (LF), neural network (NN), and wavelet least means squares (wLMS).

	LOESS	SVR	LF	NN	wLMS
LOESS	1.00	0.64	0.76	0.88	0.78
SVR	-	1.00	0.83	0.81	0.83
LF	-	-	1.00	0.87	0.99
NN	-	-	-	1.00	0.91
wLMS	-	-	-	-	1.00

The Pearson correlations of the nRMSE of the prediction filters are shown in Table 1. All the correlations are positive. The smallest correlation occurs between the LOESS and the SVR, and the highest correlation between the LF and the wLMS.

## 4 Discussion

The NN showed the smallest variation of the low nRMSE group and, therefore, performed best on this respiration data set. The prediction filters generally show high positive correlations in their nRMSE.

The high positive correlations between the low nRMSE prediction filters (see LF, NN, and wLMS in Table 1) show that if for a given respiration signal one prediction filter achieves a low nRMSE, the other prediction filters will also achieve a low nRMSE. Therefore, there are respiration signals that are easier than other respiration signals to be predicted for all prediction filters. This indicates either a general “predictability” of a respiration signal or to a similar working principle of the prediction filters.

However, it is not clear what characteristics of a respiration pattern influence the “predictability”, therefore further research into the characteristics of respiration patterns and their connections to the performances of the prediction filters is needed. Therefore, a larger variety of prediction filters need to be implemented and to be applied to a larger database of respiration signals than used in the current study.

Finally, the approach could be inverted: the patient could be guided via visual respiration feedback or audio coaching such that the patient breathes with a high “predictability” pattern. In [10], respiration data were divided up into three groups: 1) free breathing, 2) audio instruction, and 3) visual feedback. However, the authors found no difference of their prediction filter results between free breathing and their visual feedback pattern. Furthermore, this approach requires the patients to actively control their respiration in a compliant manner.

## 5 Conclusion

The performances of high performance prediction filters are similar for identical respiration signals. This indicates a general “predictability” of respiration signals, which needs to be investigated further.

### Author's Statement

**Research funding:** This work was supported by the Swiss National Science Foundation (SNSF) through “Development of prediction models for liver, lung, and breast tumors and implementation and verification of prediction filters for advanced couch tracking in a clinical environment”, Grant No. CR32I3-153491. **Conflict of interest:** Authors state no conflict of interest. **Informed consent:** Informed consent is not applicable. **Ethical approval:** The conducted research is not related to either human or animals use.

## References

- [1] Ernst F, Schlaefer A, Schweikard A. Prediction of Respiratory Motion with Wavelet-Based Multiscale Autoregression. In: Ayache N, Ourselin S, Maeder A, editors. MICCAI'07: Proc. 10th Int. Conf. on Medical Image Computing and Computer-Assisted Intervention (Brisbane, Australia). Berlin, Heidelberg: Springer Berlin Heidelberg 2007;668–675.
- [2] Ernst F, Schweikard A. Forecasting respiratory motion with accurate online support vector regression (SVRpred). International Journal of Computer Assisted Radiology and Surgery, 2009; 4:439–447.
- [3] Keall PJ, Colvill E, O'Brien R, Ng JA, Poulsen PR, Eade T, et al. The first clinical implementation of electromagnetic transponder-guided mlc tracking. Med Phys, 2014; 41:020702.
- [4] Keall PJ, Mageras GS, Balter JM, et al. The management of respiratory motion in radiation oncology report of AAPM Task Group 76. Med Phys, 2006; 33:3874–3900.
- [5] Kilby W, Dooley J, Kuduvalli G, Sayeh S, Maurer Jr C. The CyberKnife robotic radiosurgery system in 2010. Technology in cancer research & treatment, 2010; 9:433–452.
- [6] Lang S, Zeimet J, Ochsner G, Schmid Daners M, Riesterer O, Klöck S. Development and evaluation of a prototype tracking system using the treatment couch. Med Phys, 2014; 41:021720.
- [7] Murphy MJ, Dieterich S. Comparative performance of linear and nonlinear neural networks to predict irregular breathing. Phys Med Biol, 2006; 51:5903.
- [8] Ruan D, Fessler JA, Balter J. Real-time prediction of respiratory motion based on local regression methods. Phys Med Biol, 2007; 52:7137.
- [9] Speiser M, Medin P, Mao W, Papiez L, Gum F, Solberg T. First assessment of a novel IGRT device for stereotactic body radiation therapy. In: World Congress on Medical Physics and Biomedical Engineering, September 7-12, 2009, Munich, Germany. Springer, 2009;266–269.
- [10] Vedam SS, Keall PJ, Docef A, Todor DA, Kini VR, Mohan R. Predicting respiratory motion for four-dimensional radiotherapy. Med Phys, 2004; 32:2274–2283.